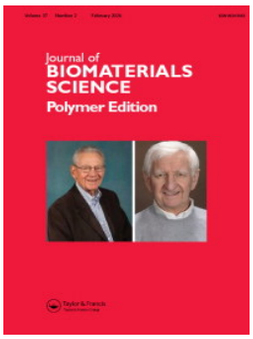

Journal of Biomaterials Science, Polymer Edition

ISSN: 0920-5063 (Print) 1568-5624 (Online) Journal homepage: www.tandfonline.com/journals/tbsp20

Plasma mediated immobilization of metformin on polyethylene: effects on drug release, antibacterial activity, and biocompatibility

Štěpán Žídek, Kateřina Štěpánková, Hana Pištěková, Milan Masař, Monika Stupavská, Pavel Sťahel, David Trunec, Miran Mozetič, Pavel Valasek & Marian Lehocky

To cite this article: Štěpán Žídek, Kateřina Štěpánková, Hana Pištěková, Milan Masař, Monika Stupavská, Pavel Sťahel, David Trunec, Miran Mozetič, Pavel Valasek & Marian Lehocky (2026) Plasma mediated immobilization of metformin on polyethylene: effects on drug release, antibacterial activity, and biocompatibility, Journal of Biomaterials Science, Polymer Edition, 37:2, 281-303, DOI: 10.1080/09205063.2025.2524261

To link to this article: https://doi.org/10.1080/09205063.2025.2524261

Published online: 03 Jul 2025.

JOURNAL OF BIOMATERIALS SCIENCE, POLYMER EDITION
2026, VOL. 37, NO. 2, 281–303
https://doi.org/10.1080/09205063.2025.2524261

Plasma mediated immobilization of metformin on polyethylene: effects on drug release, antibacterial activity, and biocompatibility

Štěpán Žídek[a], Kateřina Štěpánková[a], Hana Pištěková[a], Milan Masař[a], Monika Stupavská[b], Pavel Sťahel[b], David Trunec[b], Miran Mozetič[c], Pavel Valasek[d] and Marian Lehocky[a]

[a]Centre of Polymer Systems, University Institute, Tomas Bata University in Zlín, Zlin, Czech Republic; [b]Department of Plasma Physics and Technology, Faculty of Science, Masaryk University, Brno, Czech Republic; [c]Department of Surface Engineering, Jozef Stefan Institute, Ljubljana, Slovenia; [d]Department of Environmental Security, Faculty of Logistics and Crisis Management, Tomas Bata University in Zlín, Uherske Hradiste, Czech Republic

ABSTRACT

Metformin, a widely used antidiabetic drug, has gained attention for its potential applications in antimicrobial surfaces, delivery systems, and anticancer therapy. However, immobilizing metformin in a stable, bioactive, and dose-controllable manner onto a chemically inert, hydrophobic surface is challenging. The objective of this study is to immobilize metformin at various concentration (0.5, 1, 2, 5, 10, and 20 g·L^{-1}) onto low-density polyethylene (LDPE) surfaces by a multistep approach with the aim of creating bioactive coatings. In this approach, LDPE was first treated with a 40 kHz low pressure plasma discharge in air atmosphere, followed by non-covalent attachment of acrylic acid *via* a grafting technique. Metformin was covalently attached to the surface *via* N-(3-Dimethylaminopropyl)-N′-ethylcarbodiimide hydrochloride (EDC) and *N*-Hydroxysuccinimide (NHS) activation, while its presence on the polymer surface was confirmed by Water contact angle (WCA), Fourier transform infrared spectroscopy (FTIR) and X-ray photoelectron spectroscopy (XPS) and scanning electron microscopy (SEM). Sustained metformin release with a shift from Fickian to first-order kinetics was observed at higher drug loading. Antibacterial testing against *Staphylococcus aureus* and *Escherichia coli* showed no antibacterial effect at the selected concentration levels. Cytocompatibility assays with multipotent mesenchymal cells showed good biocompatibility of modified surfaces, with only dose-dependent cytotoxicity at higher metformin concentrations (>5 g·L^{-1}). These results demonstrate that despite the absence of antibacterial effects, the developed system offers a promising platform for further biomedical applications requiring controlled drug surface functionalization and retained cytocompatibility.

ARTICLE HISTORY
Received 5 December 2024
Accepted 16 June 2025

KEYWORDS
Antibacterial coating; surface modification; plasma treatment; metformin; diabetes

CONTACT Kateřina Štěpánková stepankova@utb.cz Centre of Polymer Systems, University Institute, Tomas Bata University in Zlín, Trida Tomase Bati 5678, Zlin, 760 01, Czech Republic

1. Introduction

Drug repurposing refers to the identification of novel therapeutic applications for existing drugs, whether already approved or under investigation, that extend beyond their initially intended medical indications [1]. The development of drug repurposing focuses on identifying novel therapeutic indications for approved pharmaceuticals or bioactive agents, whether synthetic or naturally sourced, in advanced preclinical research [2]. This strategy significantly reduces the time, costs, and risks inherent in traditional drug discovery pipelines, as the compounds involved have already been de-risked through prior safety and toxicity assessments, offering a streamlined path toward clinical application [3].

One prominent candidate in drug repurposing efforts is metformin (dimethylbiguanide), FDA approved since 2002 [4] and widely used antihyperglycemic medication and first-line treatment for patients with type 2 diabetes mellitus [5]. Several studies indicate that diabetic patients on metformin have a reduced incidence of infections, implying a potential antimicrobial effect of the drug [6–8]. A recent study found that metformin, a non-antibiotic drug, exhibited a synergistic effect with doxycycline against *Shigella boydii*, showing promise as an adjuvant to enhance antibiotic efficacy in both *in vitro* and *in vivo* tests [9]. The combination of metformin with other conventional antibiotics, such as levofloxacin, ampicillin, chloramphenicol, and rifampicin exhibited additive effects against methicillin-resistant *Staphylococcus aureus* and multidrug-resistant *Pseudomonas aeruginosa* [10]. The antibacterial properties of metformin remain a subject of ongoing research. Metformin appears to engage multiple biological mechanisms, including modulation of the immune response to infections, enhancement of antibiotic efficacy, and disruption of bacterial outer membranes and efflux pumps [11–13]. Numerous clinical trials have demonstrated that metformin has inhibitory effects on tumor growth, invasion, and metastasis [14–16]. Metformin is also effective in treating osteoarthritis [17], inflammation [18], endometriosis [19], vascular disease [20], musculoskeletal disorders [21], and venous thrombosis [22].

In this context, the modification of polymeric surfaces with bioactive compounds, such as metformin represents an innovative approach to localized drug delivery, antibacterial, and implant coatings [23–26]. Plasma-assisted surface functionalization offer a versatile platform for the deposition of various bioactive molecules onto polymeric substrates, thereby enabling controlled release and localized therapeutic response [27,28]. This approach has been used to create functionalization gradients that control adsorption and release of therapeutic agents, making it valuable for controlled drug delivery systems, such as dermal patches, microcapsules, and bioactive coatings [29].

Plasma treatment of polymeric materials using air as a carrier gas is a highly effective method for facilitating the incorporation of oxygen-containing functional groups, such as hydroxyl (–OH), carboxyl (–COOH), and carbonyl (–CO) groups to polymeric surfaces [30]. Certain functional groups exhibit instability, leading to subsequent reactions that generate highly reactive radicals. These metastable species can engage in further reactions with appropriate monomers, resulting in the formation of polymeric 'brush-like' structures [31]. A rather comprehensive review on the surface effects of plasma treatment of polyethylene was published [32]. It should be noted that the surface hydrophilization of this polymer by a common plasma treatment is not stable but

numerous authors reported rather fast hydrophobic recovery. Furthermore, even a brief exposure to liquids may cause a quick loss of the hydrophilicity [33]. Acrylic acid serves as an excellent source of carboxyl-rich (–COOH) groups, making it ideal for grafting with a thin film of different organic materials. Such configurations are ideal for interactions with bioactive agents through the formation of intermolecular forces, thereby enhancing surface functionality and compatibility [34].

In recent years, diverse multistep biomolecule surface immobilization strategies have been explored to impart antibacterial and other biofunctionalities to polymer substrates, including plasma-induced monomer grafting [34], chemical grafting [35], physical adsorption [36], host-guest chemistry [37], layer-by-layer assembly [38], plasma electrolytic oxidation [39], catechol-assisted immobilization [40], and many others. For instance, Hast et al. developed a novel surface functionalization method based on tyrosinase-catalyzed polymerization of a catecholamine (DOPA-Tet), enabling subsequent bio-orthogonal grafting of various bioactive molecules, such as enzymes, peptides, and antibiotics under physiological conditions, while maintaining their bioactivity and cytocompatibility [41]. In another approach, positively charged polymer brushes were formed on plasma-treated LDPE surfaces *via* vapor-phase grafting of allylamine-based monomers, enabling subsequent immobilization of chondroitin sulfate for enhanced bioactivity [42]. Liu et al. reported a dual pH- and thermo-responsive polymeric micelles based on host–guest interactions were engineered using benzimidazole-modified graft copolymers and β-cyclodextrin-based star block copolymers, enabling efficient drug loading and controlled release of doxorubicin with excellent antitumor efficacy [43].

Despite extensive research on surface functionalization and drug repurposing, the covalent bonding of metformin to polymer substrates using this multistep strategy remains unexplored.

This study aims to investigate the feasibility of immobilizing metformin onto LDPE surfaces as a model polymer containing only carbon and hydrogen atoms through a multistep physico-chemical process involving plasma treatment. Apart from plasma surface functionalization, acrylic acid was grafted onto the reactive sites of the polymer surface facilitating the formation of covalent bonding between the carboxyl groups of acrylic acid and the amine groups of metformin *via* carbodiimide chemistry. Surface hydrophilicity and surface energy analysis was carried out by measuring the static contact angle of droplets with different surface tensions, chemical analysis was performed by X-ray photoelectron spectroscopy and FTIR, and surface morphology was investigated with a scanning electron microscope. Antibacterial performance of the samples was tested against *S. aureus* (CCM 4516) as Gram-positive and *Escherichia coli* (CCM 4517) as Gram-negative representatives. Finally, *in vitro* cytocompatibility of the samples was studied using multipotent mesenchymal cells.

2. Materials and methods

2.1. Materials and reagents

Low-density polyethylene (LDPE) films made from Borstar FB4230 pellets (Borealis AG, Vienna, Austria) with dimensions of 50 × 50 mm were used as a substrate for deposition.

Acrylic acid (99%), sodium metabisulfite (99%), and sodium hydroxide (98%), supplied by Sigma-Aldrich (St. Louis, MO, USA) were incorporated into the grafting process. 1,1-Dimethylbiguanide hydrochloride (metformin), N-(3-Dimethylaminopropyl)-N'-ethylcarbodiimide hydrochloride (EDC) 98% and N-Hydroxysuccinimide (NHS) 98% (Sigma-Aldrich, St. Louis, MO, USA) were employed in the deposition. Deionized water, diiodomethane (99.0%, reagent plus) and formamide (99.5%, molecular biology grade) (Sigma-Aldrich (St. Louis, MO, USA) were used for surface energy measurement. Antibacterial tests were done with bacterial strains of *S. aureus* (CCM 4516) and *E. coli* (CCM 4517).

2.2. Plasma hydrophilization and deposition protocol

Metformin was deposited onto a polymeric carrier from LDPE *via* multistep physico-chemical process, as depicted in Figure 1. This process involved treating the surface using a low-pressure air plasma. Plasma treatment was performed in high frequency (40 kHz) plasma reactor Diener Pico (Diener Electronic GmbH & Co. KG, Nagold, Germany). A sample was placed into the plasma reactor, which was evacuated to reach an ultimate pressure of 10 Pa. Then, air was introduced into the plasma reactor during continuous pumping, and the flow rate was set to 20 sccm. The gas pressure during plasma treatment was 50 Pa. The plasma treatment conditions were selected based on previously reported protocols that demonstrated effective surface activation of LDPE without causing thermal or oxidative degradation [44]. The samples were exposed to plasma from both sides for 1 min at a power of 50 W. After, the acrylic acid (AA) was grafted onto the plasma-activated surface of the polymer film. This process was carried out in a solution of 10% acrylic acid (AA) and sodium metabisulfite for 24 h. The AA carboxylic groups then serve as centers for the adhesion of the active substance, i.e. metformin. Then, the films were immersed in a 1% NaOH solution to neutralize and terminate the polymerization process. Before

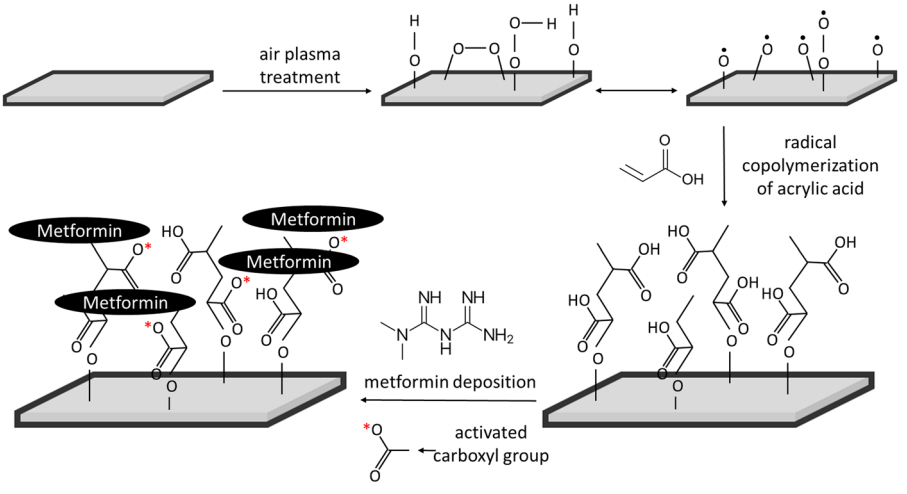

Figure 1. Schematic representation of plasma post-irradiation grafting of AA onto a PET surface followed by immobilization of metformin.

metformin deposition, the samples were further immersed in EDC/NHS solution for 4 h to activate the acrylic acid carboxyl groups. In our case, aqueous solutions of metformin were prepared at concentrations of 0.5, 1, 2, 5, 10, and 20 $g \cdot L^{-1}$. Correspondingly, the specimens are labeled as LDPE REF (untreated), LDPE PL (plasma-treated), LDPE grafted with acrylic acid (AA), and MET 0.5 to MET 20 for LDPE samples with increasing concentrations of deposited metformin. The amino group of metformin forms an amide bond with the original carboxyl group of AA, and the by-product of the reaction is released as a urea derivative. After removal from the metformin solution, the samples were rinsed with deionized water and left to dry under laboratory conditions. The surface characterization and biological evaluation of the prepared samples were then carried out.

2.3. Surface characterization of prepared films

The FTIR spectra of prepared modified surfaces were obtained *via* Fourier transform infrared spectroscopy (FTIR) using Nicolet iS5 (Thermo Scientific, Grand Island, NY, USA) equipped with iD5 attenuated total reflectance (ATR). FTIR spectra were collected in the range of 600–4000 cm^{-1} with a resolution of 2 cm^{-1} and 64 scans using a germanium crystal at an incident angle of 45°.

The water sessile drop contact angle method was performed to evaluate the wettability of prepared modified surfaces using SEE system (Advex Instruments, Brno, Czech Republic). From the measured values of the contact angles of various droplets, the surface free energy of each sample was determined using Lewis acid-base parameters. Deionized water, formamide, and diiodomethane were selected as suitable liquids for evaluation of the surface free energy. For each liquid, five individual measurements were taken and averaged to provide representative contact angle values, which were then used to calculate the surface free energy for each sample. Droplets of 5 µL of each test liquid were applied to the samples and recorded with a CCD camera. All data points are means of a minimum of 3 independent experiments, each of 5 replicates. The data are expressed as mean ± *SD*.

XPS was used to characterize the chemical composition of the prepared surfaces, which in our case was performed on an ESCALAB 250Xi device (Thermo Fisher Scientific, East Grinstead, United Kingdom). Using this method, we were able to obtain information on the percentage of chemical elements on the samples. The samples were exposed to X-ray beam with power of 200 W (650 microns spot size). The survey spectra were acquired with a pass energy of 50 eV and energy step of 1 eV. In order to compensate for charges on the surface, an electron flood gun was used. Spectra calibration, processing, and fitting routines were done using the Avantage software (v.5.9925). XPS measurements were performed on three independently prepared samples per condition. For each sample, three different spots were analyzed and averaged. The data are expressed as mean ± *SD*.

The surface morphology of each sample was examined using a NANOSEM 450 scanning electron microscope (FEI, Thermo Fisher Scientific, Hillsboro, OR, USA) equipped with an energy-dispersive X-ray spectroscopy (EDX) analyzer. Elemental analysis was performed using a high-sensitivity Circular Backscatter Detector (CBS),

operated at 15 kV with a spot size of 3.5. Prior to observation, the samples were coated with a conductive thin layer of Au/Pd. SEM images were acquired at a magnification of 10.000×.

2.4. In-vitro drug release test

In vitro drug release kinetics of MET from EDC/NHS-crosslinked films were studied in phosphate-buffered saline (PBS, pH 7.4) at 37 °C to simulate physiological conditions. LDPE films with a surface area of 2.5 cm^2 were immersed in 10 mL of PBS and placed on an oscillating shaker at 150 rpm. At predetermined time intervals, 1 mL aliquots were withdrawn and replaced with an equal volume of fresh medium. After appropriate dilution, the concentration of released metformin was quantified using a UV–Vis spectrophotometer (PerkinElmer Lambda 1050, PerkinElmer Inc., USA) by monitoring the characteristic absorbance peak at λ_{max} = 233 nm. All experiments were conducted in triplicate, and the data are expressed as mean ± *SD*.

The drug loading efficiency of the functionalized LDPE films was assessed by quantifying the amount of metformin loaded per unit area of the films. Films with an area of 2.5 cm^2 were incubated in 10 mL of PBS under oscillation for 24 h. The absorbance of the withdrawn solution (1 mL) was measured at λ_{max} = 233 nm, and the metformin content was calculated using the corresponding calibration curve ($y = 0.0851x + 0.0092$, $R^2 = 0.9991$).

To elucidate the release mechanism of metformin hydrochloride from LDPE films, various kinetic models—including Korsmeyer–Peppas, Higuchi, zero-order, and first-order—were applied. The model yielding the highest coefficient of determination (R^2) was deemed the most appropriate, offering the best fit to the experimental release data.

2.5. Evaluation of antibacterial activity of films

Before antibacterial testing, the samples prepared according to the multistep process described above were disinfected by UV radiation, while polypropylene foils were cleaned before the plasma treatment by rinsing with 70% denatured ethanol. Two bacterial strains were used for the evaluation of antibacterial activity: gram-negative *E. coli* CCM 4517 and gram-positive *S. aureus* CCM 4516. The antibacterial tests were conducted in accordance with ISO 22196, with some modifications. Bacterial suspensions of *E. coli* (3.4×10^5 CFU·mL^{-1}) and *S. aureus* (1.2×10^5 CFU·mL^{-1}) were prepared using 1/500 Nutrient broth (HiMedia Laboratories, India). A 100 µL volume of the bacterial suspension was applied to the sample surface (25 × 25 mm), which was then covered with a polypropylene foil (20 × 20 mm). This corresponds to a volume-to-surface area ratio of 0.25 µL·mm^{-2}, ensuring even distribution of bacteria over the test surface. The samples thus prepared were incubated at 35 °C with 100% relative humidity for 24 h. After incubation, the polypropylene foils were removed, and each sample was thoroughly neutralized by rinsing with SCDLP broth (HiMedia Laboratories, India), which was subsequently collected. The number of viable bacterial cells was determined *via* the pour plate culture method (PCA, HiMedia Laboratories, India). Measurements were performed in triplicate.

2.6. Evaluation of cytocompatibility

In vitro cytotoxicity was evaluated using the MTS assay, which measures mitochondrial activity in living cells by converting a tetrazolium salt into a colored formazan. The amount of formazan produced correlates with the number of viable cells and is detected spectrophotometrically at 490 nm. For this study, D1 cells (multipotent mesenchymal cells (MSCs), American Type Culture Collection, Manassas, VA, USA), cloned from BALB/c mouse bone marrow cells, were selected as a representative MSC model due to their well-established capacity for rapid osteogenic differentiation *in vitro* [45,46]. The cells were cultured in Dulbecco's Modified Eagle's Medium (Invitrogen, Carlsbad, CA, USA) containing 10% fetal bovine serum and 0.1% sodium ascorbate, maintained in a humidified atmosphere of 5% CO_2 at 37 °C. The cells were seeded on virgin PET and PET substrates coated with pentane and hexane plasma polymers in 24-well plates at a density of 100,000 cells per well. After 48 h, cell proliferation was assessed using the MTS tetrazolium (3-(4,5-dimethylthiazol-2-yl)-5-(3-carboxymethoxyphenyl)-2-(4-sulfophenyl)-2H-tetrazolium) (CellTiter 96 Aqueous Non-Radioactive Cell Proliferation Assay kit, Promega, Madison, WI, USA). Three hours before the end of the incubation period, 10 µL of MTS reagent was added to each well, and cells were incubated for an additional 3 h at 37 °C. Absorbance was then measured at 490 nm using a microplate reader EL800 Universal Microplate Reader (BioTek Instruments, Winooski, VT, USA). The experiment was repeated three times, and the results were expressed as a percentage of cell viability compared to control. The mean absorbance of cells grown without PET or PET with pentane and hexane plasma polymers was used to calculate 100% cellular viability. Cytotoxicity was categorized based on the percentage of cell viability: values above 75% were considered non-cytotoxic, 75–50% indicated weak cytotoxicity, 50–25% represented moderate cytotoxicity, and below 25% signified strong cytotoxicity. The cytotoxicity data are presented as mean values with standard errors of the mean from a minimum of three independent experiments conducted in triplicate. Statistical analysis was performed using Student's *t*-test to assess differences between experimental groups, with significance defined as $p < 0.05$.

3. Results and discussion

3.1. Functional groups identification by FTIR analysis

FTIR was employed to investigate the chemical structure of the modified LDPE surfaces and confirm the successful deposition of metformin. The spectra were measured for LDPE REF, LDPE PL, LDPE grafted with AA, and MET 0.5–MET 20. Additionally, the spectrum of pure metformin (MET) was used as a reference.

In the FTIR spectrum of untreated LDPE (LDPE REF), the characteristic peaks of LDPE are observed at wavenumbers 2917 and 2848 cm^{-1} (Figure 2), corresponding to the vibrations of the CH_2 groups. Additional peaks at 1471 and 719 cm^{-1} are also attributed to the vibrations of the CH_2 groups. These peaks remain visible in all subsequent spectra, indicating that the base polymer structure remains intact throughout the modification process. It is important to note, however, that FTIR is not highly surface-sensitive and predominantly detects bulk properties. The spectrum of

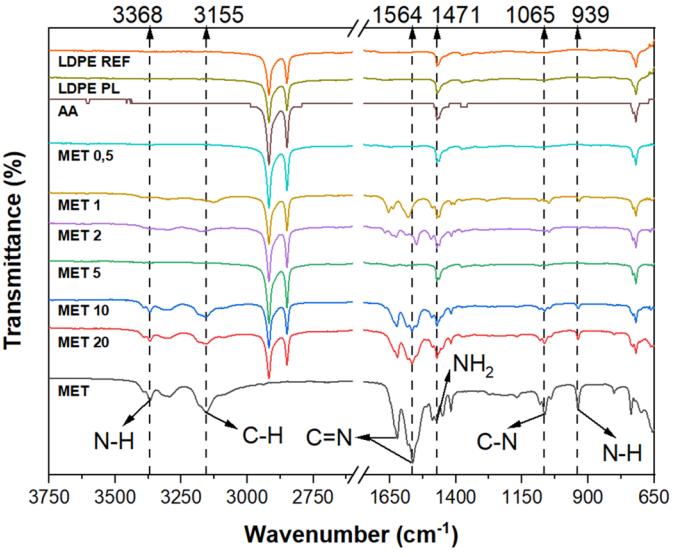

Figure 2. Attenuated total reflectance (ATR)-FTIR spectrum collected from the samples: spectrum LDPE REF stands for pure LDPE, which was used as a reference, spectrum LDPE PL is for LDPE treated with plasma in air, spectrum AA is for LDPE with bonded AA, spectra MET 0.5–20 stands for LDPE with deposited metformin in concentrations of 0.5–20 g·L^{-1} and spectrum MET is for pure metformin powder.

plasma-treated LDPE (LDPE PL) shows no significant differences compared to the untreated LDPE. This is consistent with the fact that plasma treatment primarily induces surface oxidation without creating detectable new bulk chemical bonds. The oxidative functional groups introduced by plasma treatment are often present in quantities too low to be clearly identified by FTIR, especially when thin layers are involved. For the acrylic acid-grafted sample (AA), the spectrum also remains largely similar to the untreated LDPE, with no new discernible peaks. This can be attributed to the relatively thin layer of AA grafted onto the surface, which may be below the detection limit of the FTIR spectrometer.

The most significant changes in the FT-IR spectra are observed after metformin deposition. In the sample with a metformin concentration of 1 g·L^{-1} (MET 1), characteristic peaks of metformin start to emerge. Notably, a peak at 3368 cm^{-1} is attributed to the N–H stretching vibration, and a peak at 3155 cm^{-1} corresponds to the C–H vibration. Additionally, distinct peaks at 1622 and 1564 cm^{-1} are assigned to the vibrations of the C = N bond, while peaks in the region of 1420–1470 cm^{-1} correspond to the vibrations of the NH_2 group. These peaks confirm the successful deposition of metformin on the polymer surface. As the concentration of metformin increases, the intensity of these characteristic peaks also increases, indicating the presence of higher quantities of metformin on the surface. In the sample with the highest concentration (MET 20), the peaks associated with metformin functional groups are most pronounced, particularly the N–H stretching at 3368 cm^{-1} and the C–N stretching at 1065 cm^{-1}. The peak at 939 cm^{-1}, corresponding to the N–H vibrations, is also evident, further confirming the successful immobilization of metformin. The results are in accordance with other studies [47,48]. Interestingly, the sample with 5 g·L^{-1}

metformin (MET 5) did not exhibit strong characteristic peaks of metformin, which may suggest heterogeneous deposition or incomplete coverage at this concentration. This irregularity could be due to variability in the surface interactions or metformin layer thickness, which affects the spectroscopic detection of metformin functional groups.

3.2. Surface wettability and surface energy analysis

Surface wettability and energy are key parameters that help understand the success of surface modifications, especially in biomedical applications, as they influence interactions with biological environments. In this study, the wettability of the prepared LDPE surfaces was evaluated using the water sessile drop contact angle method, while surface free energy was determined by using two additional liquids and calculated using Lewis acid-base theory [49]. Three test liquids—deionized water, formamide, and diiodomethane—were used to measure contact angles and calculate the surface energy. The measured contact angles of the different fluids are shown in Figure 3.

The contact angle of pure LDPE (LDPE REF) with deionized water was 82.6°, indicating a rather hydrophobic surface. This hydrophobicity, reflected in the low surface energy of 38.2 $mJ \cdot m^{-2}$ (Table 1), is typical of untreated polyolefins, which lack surface reactivity and are unsuitable for subsequent chemical modifications [50]. However, plasma treatment (LDPE PL) significantly altered the surface wettability. The water contact angle dropped to 57.0°, demonstrating a significant increase in hydrophilicity. This change is attributed to the introduction of polar functional groups onto the polymer surface during plasma treatment [32]. Consequently, the surface free energy increased to 49.5 $mJ \cdot m^{-2}$, making the surface more favorable for further chemical functionalization.

Subsequent grafting with AA resulted in a slight increase in the contact angle to 62.0°, while the surface energy decreased to 42.2 $mJ \cdot m^{-2}$. This is a typical value for

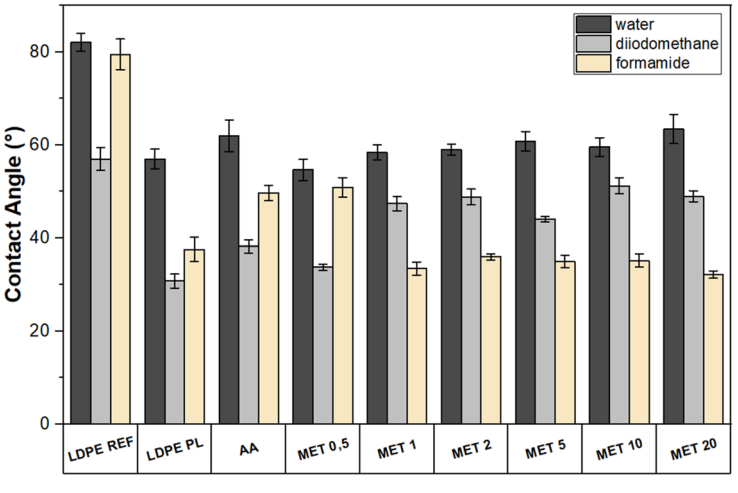

Figure 3. Contact angles of the liquids used on the surfaces of the prepared samples.

Table 1. Surface free energy of the prepared samples.

Sample	γ_s	γ_s^{LW}	γ_s^{AB}	γ_s^+	γ_s^-
LDPE REF	38.2	30.3	7.9	1.0	16.2
LDPE PL	49.5	43.9	5.6	0.4	19.2
AA	42.2	40.5	1.7	0.1	20.4
MET 0.5	46.2	42.6	3.6	0.1	32.0
MET 1	43.5	42.9	0.6	0.0	23.7
MET 2	42.3	41.6	0.7	0.0	23.9
MET 5	46.0	42.1	3.9	0.2	18.3
MET 10	43.2	41.9	1.3	0.0	24.9
MET 20	44.0	43.3	0.7	0.0	18.2

hydrophilic polymers with a large concentration of oxygen [51]. The somehow higher water contact angle compared to the plasma-treated surface is thus explained by the thermally non-equilibrium state of the freshly plasma-treated polyethylene as compared to thermodynamically stable AA. The presence of polar functional groups (such as carboxyl does not necessarily lead to a better adhesion of a coating [52], but the carboxyl groups are likely to interact with amino groups from a deposited material to form a covalent bond [35].

The deposition of metformin onto the AA-modified polyethylene surface further modified the water contact angle. At a metformin concentration of 0.5 g·L^{-1} (MET 0.5), the contact angle decreased to 54.7°, reflecting a more hydrophilic surface. This effect is difficult to explain because increasing the concentration of deposited metformin caused a gradual decrease in wettability (increase in the WCA) with increasing metformin concentration (Figure 3). For metformin concentrations of 1 g·L^{-1} and higher (MET 1 to MET 20), the contact angle values ranged from 60.0 to 63.4°, with only minor variations. The measured surface free energy values (Table 1) corroborate this behavior, with the highest surface energy observed at lower metformin concentrations (46.2 mJ·m^{-2} for MET 0.5) and a slight decrease at higher concentrations. This trend may indicate that the metformin layer reaches an equilibrium state, where additional deposition no longer contributes to changes in surface energy or wettability [53].

Based on the experimental results, it can be concluded that the plasma treatment introduced hydrophilic functional groups, while AA provided reactive carboxyl sites for metformin attachment. Metformin deposition on polyethylene substrates may be useful in biomedical applications where wettability and surface energy play critical roles in biological interactions [54].

3.3. Chemical composition analysis: XPS results

XPS was used to determine the chemical composition of the prepared LDPE surfaces at various stages of the modification process. The results are summarized in Table 2, which shows the percentage of carbon (C), oxygen (O), and nitrogen (N). The concentration of trace elements including sulfur (S), silicon (Si), and chlorine (Cl) was well below 1%. These elements are critical indicators of the surface modification success, as metformin deposition introduces nitrogen, while plasma treatment and AA grafting alter the oxygen concentration.

Table 2. Elemental analysis of the prepared samples.

	Atomic percentage (%)		
Sample	C	O	N
LDPE REF	97.6	2.4	0.0
LDPE PL	85.8	11.7	2.5
AA	89.2	9.0	1.8
MET 0.5	87.6	10.1	2.3
MET 1	87.2	9.2	3.6
MET 2	89.0	8.9	2.2
MET 5	88.3	8.0	3.7
MET 10	88.2	7.3	4.5
MET 20	82.0	8.9	9.1

The XPS analysis of untreated LDPE (LDPE REF) revealed a high carbon content (97.6%) with small amounts of oxygen (2.4%), consistent with the chemical structure of the base polymer. The small concentration of oxygen is often observed in XPS spectra of polyolefins and is often attributed to impurities [32]. Plasma treatment (LDPE PL) significantly altered the surface composition, decreasing carbon levels to 85.8% and increasing oxygen to 11.7%. This increase in oxygen content is attributable to the formation of oxidative functional groups during plasma exposure, which is crucial for enhancing the surface reactivity for subsequent chemical modifications [55]. Here, the final depth resolution of XPS should be mentioned. The concentration of oxygen on the surface is probably larger, but the escape depth of photoelectrons arising from carbon or oxygen C1s spectra is several nm, so XPS averages the concentration over the surface film. Nitrogen also appears in the survey spectra of plasma-treated polyethylene because of the presence of reactive nitrogen species in the air plasma. Following AA grafting, the oxygen content slightly decreased to 9.0%, with a corresponding minor increase in nitrogen content (1.8%). This observation is difficult to explain taking into account the composition of acrylic acid (40 at.% O and 60 at.% C). One feasible explanation is the loss of plasma-induced polar groups upon incubation in the liquid [56], and a trivial explanation is formation of a unevenly distributed and/or very thin film of AA so that the surface composition as probed by XPS is within the limits of the experimental error.

The metformin-modified samples showed a gradual increase in nitrogen content with increasing metformin concentration. For instance, the sample with 0.5 $g \cdot L^{-1}$ of metformin (MET 0.5) exhibited 2.3% nitrogen, which rose to 9.1% in the sample with 20 $g \cdot L^{-1}$ of metformin (MET 20). This trend confirms that metformin, which contains nitrogen in its molecular structure, was successfully deposited onto the LDPE surface. Concurrently, the oxygen content decreased from 10.1% (MET 0.5) to 8.9% (MET 20), indicating that the surface functional groups created during plasma treatment were gradually covered by the metformin layer as its concentration increased. This trend is also summarized in the following graph (Figure 4), where we can see the percentage of oxygen (O) and nitrogen (N) on the investigated samples. Still, the oxygen persistence in all XPS spectra indicates that the metformin film is either thinner than the escape depth of O1s photons or the film does not cover the surface entirely. A trivial explanation will be the existence of the surface impurities like water molecules which has not desorbed entirely when placing the samples to the ultra-high vacuum conditions in the XPS chamber.

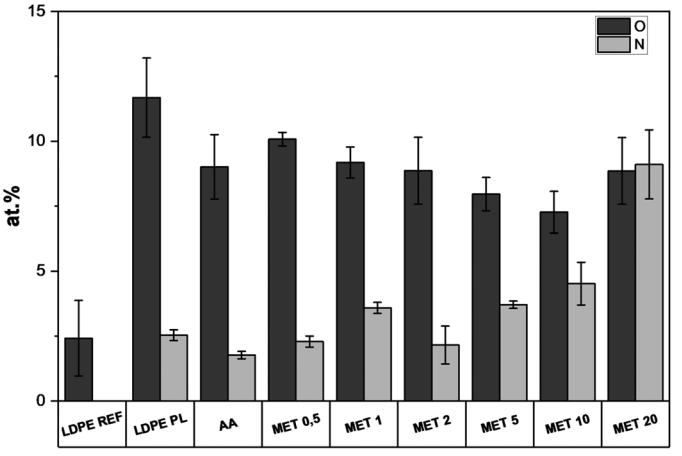

Figure 4. Percentage of oxygen (O) and nitrogen (N) on prepared samples. The data represent means ± *SD*.

3.4. The surface morphology analysis

The SEM micrograph of the untreated LDPE surface (Figure 5(A), top) reveals a smooth, homogeneous morphology devoid of discernible topographical features, indicative of an unmodified and inert polymeric surface. This observation is corroborated by the accompanying EDX spectrum (Figure 5(B), top), which confirms the material's elemental purity, with carbon constituting 99.62 at.%. Only trace amounts of gold and palladium were detected, likely originating from sputter coating.

A marked difference is observed in the SEM image of LDPE following metformin deposition (Figure 5(A), bottom) demonstrating a pronounced alteration in surface morphology. The emergence of stratified or flake-like structures, along with increased surface roughness (as denoted by the yellow arrow), illustrates a gradual transition from uncoated LDPE to metformin-covered regions, indicative of effective surface immobilization through a continuous yet spatially heterogeneous deposition. This morphological change is further supported by EDX analysis (Figure 5(B), bottom), which indicates a reduction in carbon content to 81.65 at.% and the introduction of nitrogen and oxygen, elements consistent with the molecular structure of metformin.

While LDPE provides a chemically inert baseline, the incorporation of metformin imparts surface heterogeneity and microstructural complexity, potentially enhancing the specific surface area and promoting favourable biointerfacial interactions, particularly in cell adhesion. However, excessive surface loading at higher metformin concentrations may result in aggregation or overcoating, possibly compromising cytocompatibility, as evidenced in Figure 6.

3.5. In vitro drug release test

The *in vitro* release profiles of MET in three representative concentrations from LDPE films are presented in Figure 6. The release profiles exhibited a biphasic pattern: a rapid initial release, followed by a plateauing sustained release. The burst release, especially in MET 20 and MET 5, is attributable to loosely bound or physisorbed

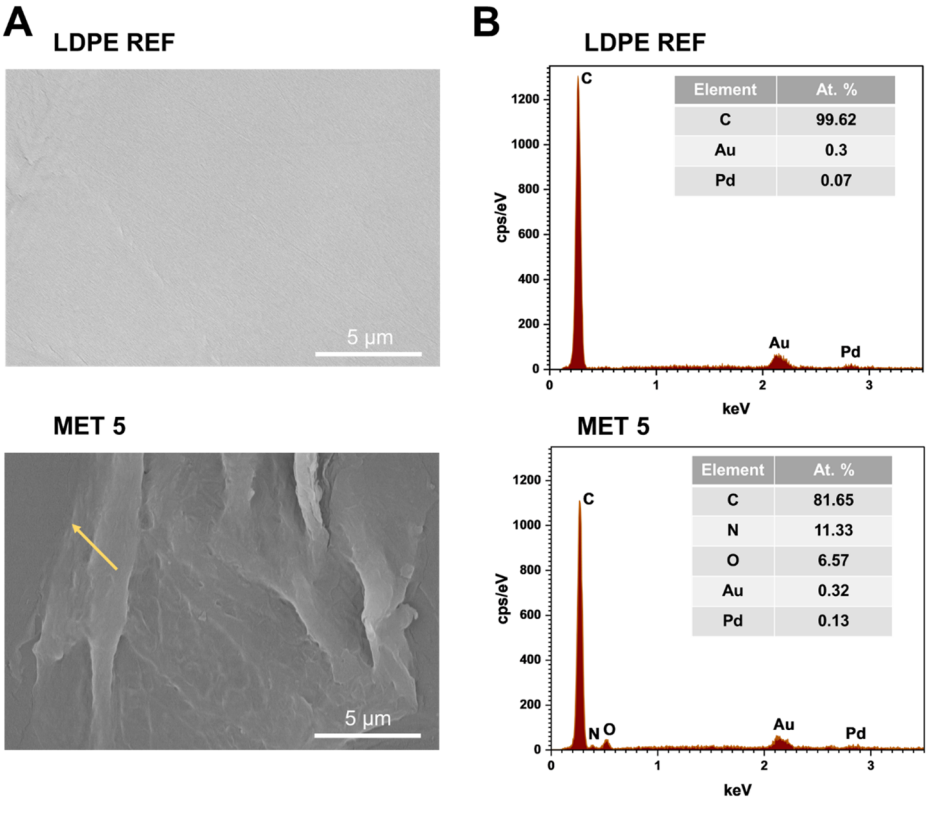

Figure 5. (A) SEM images of LDPE surfaces: untreated (top left) and treated with metformin (5 g·L^{-1}, bottom left). (B) EDX spectra showing the chemical composition of untreated and metformin-treated LDPE surfaces with corresponding atomic percentages of detected elements.

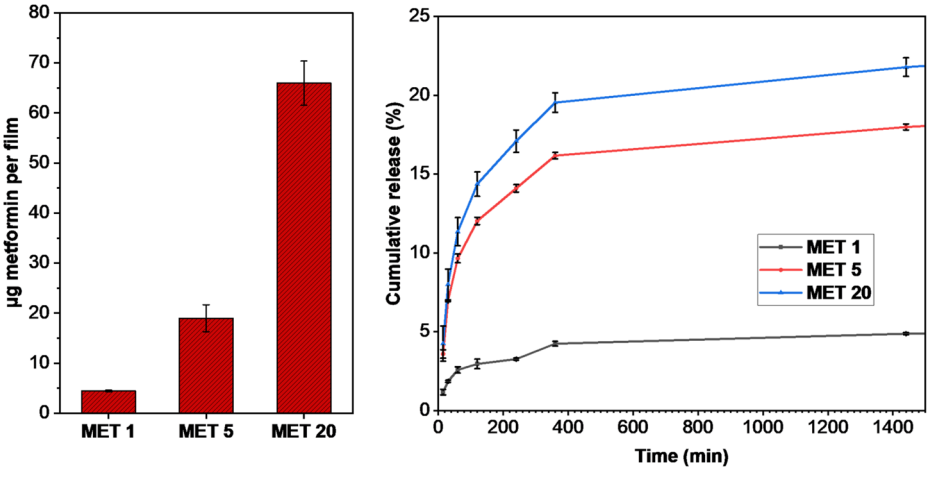

Figure 6. Drug loading and release profiles of metformin from LDPE films using three representative concentrations (MET 1, MET 5, and MET 20). Left: loading capacity; right: cumulative release in PBS. Data represent mean ± *SD*.

metformin molecules and/or to the release of the drug near the LDPE surface which is a routine phenomenon among polymer-based matrixes [57]. The slower phase likely corresponds to diffusion from the polymer network or partial hydrolysis of labile amide/ionic interactions. The release plateau observed after 300 min is consistent with diffusion-limited systems, yet notably higher release efficiencies (up to 22%) compared to unmodified LDPE systems reported in literature underscore the role of surface functionalization in enhancing drug availability. Despite the improved release, the total cumulative release remained moderate, likely due to the presence of immobilized metformin, which was covalently or ionically bound to carboxyl-modified surfaces and not readily diffusible. This is supported by similar systems where EDC/NHS activation led to strong drug immobilization, reducing free diffusion into the medium [35]. The relatively low release from MET 1 highlights the limitation of achieving therapeutic release levels from films with minimal loading, despite prolonged exposure. Drug loading (Figure 7, left) increased proportionally with the concentration of metformin used during incubation, with MET 20 reaching up to ~72 µg per film. This is attributed to the enhanced hydrophilicity and chemical reactivity of the functionalized LDPE surface, which likely increased drug retention capacity.

The mechanism of drug release for different concentrations of bounded metformin was investigated using various kinetic models, and the results were presented in Table 3. The best fit for the highest value of the regression coefficient (R^2) provides the release model. The best fitting model to the MET 1 release was observed using Korsmeyer–Peppas model (R^2 = 0.9386), with a diffusion exponent $n \geq 0.45$, indicative of Fickian diffusion, where the diffusion-controlled release rate of drug molecules

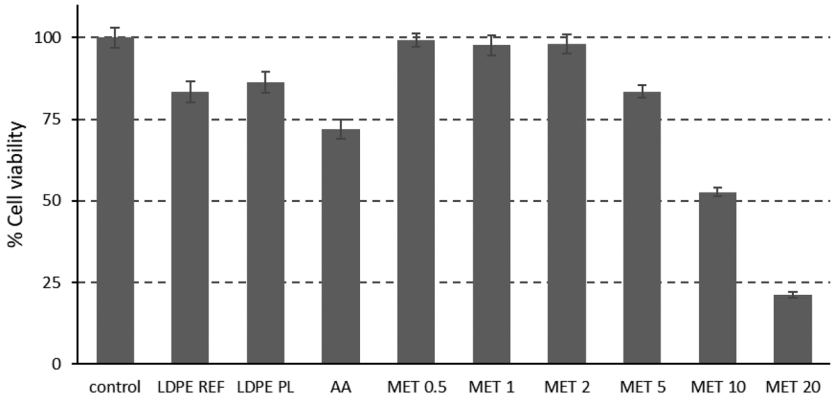

Figure 7. Cell viability of tested samples. Values above 75% were considered non-cytotoxic, 75–50% indicated weak cytotoxicity, 50–25% represented moderate cytotoxicity, and below 25% signified strong cytotoxicity. The data represent means ± *SD*.

Table 3. R^2 value of drug release from samples with different metformin concentration.

	Zero order	First order	Higuchi	Korsmeyer-Peppas	
Sample	R^2	R^2	R^2	R^2	n
MET 1	0.5216	0.5276	0.7546	0.9386	0.24
MET 5	0.4939	0.9654	0.727	0.8386	0.28
MET 20	0.5058	0.9501	0.7382	0.8483	0.29

decreases as a function of time due to a reduction in the concentration gradient [58]. Drug release data were fitted well in the first-order kinetic model for MET 5 and MET 20. First-order kinetic model can be successfully used to describe drug release from polymeric films indicating that drug release mechanism is concentration dependent. The amount of drug release decreases with decreasing concentration gradient over time [59]. The release kinetic studies revealed that as the loading of drug in the LDPE increased, the concentration of the drug released also increased. Similar to previously reported systems in which metformin exhibited first-order release kinetics due to its preferential localization near the polymer surface rather than homogeneous distribution within the matrix [60], the present LDPE-based films likely promote concentration-dependent release governed predominantly by surface-associated drug diffusion. This surface enrichment of metformin, combined with partial covalent or ionic immobilization to carboxyl-functionalized sites, violates the assumptions of the Higuchi model, which presumes uniform drug dispersion and purely Fickian diffusion from a homogenous matrix. Although kinetic modeling supports diffusion-controlled release, the total release of only 22% over 24 h suggests limited diffusional mobility of metformin through the LDPE matrix. This restricts the system's suitability for systemic drug delivery but highlights its potential for localized, surface-mediated therapeutic applications where low-dose, sustained release is sufficient.

3.6. Evaluation of antibacterial activity of films

The antibacterial activity of the prepared films was assessed based on the ISO 22196 standard, with some modifications to suit our experimental setup. In particular, two bacterial strains were selected for the evaluation: a Gram-negative *E. coli* (CCM 4517) and Gram-positive *S. aureus* (CCM 4516). These strains were chosen due to their relevance in healthcare-associated infections and the need to explore the potential of metformin-treated surfaces for antimicrobial applications.

Table 4 summarizes the exact viable cell counts on the sample surfaces after 24 h of incubation, along with the antibacterial effectiveness (R values) based on colony-forming units (CFU/cm^2). The reproducibility of these results was rather low, because the statistical error was up to an order of magnitude. The results indicate that, overall, the samples did not exhibit any antibacterial activity. In both *E. coli* and *S. aureus* assays, the number of viable bacterial cells post-incubation on metformin-covered samples was equal to or higher than those observed on the reference LDPE surface (LDPE REF). This suggests that the surface modifications introduced through plasma pre-treatment and metformin deposition were insufficient to confer meaningful antibacterial properties. Interestingly, there was a slight trend of higher antibacterial effectiveness against *E. coli* at lower metformin concentrations, particularly in the MET 0.5 and MET 1 samples. However, this effect diminished as the concentration increased, and the antibacterial activity against *E. coli* was virtually absent in samples with metformin concentrations of 2 g·l^{-1} and above. Furthermore, the only statistically significant antibacterial effect against *E. coli* is observed for the sample treated with plasma only. Despite these observations, the

Table 4. Viable bacteria numbers on the surface of the prepared samples; antibacterial effect (R) values are expressed in CFU.

	Staphylococcus aureus CCM 4516		*Escherichia coli* CCM 4517	
Sample	N (CFU/cm^2)	R	N (CFU/cm^2)	R
LDPE REF	2.5×10^4	$U_t=4.4$	4.6×10^5	$U_t=5.7$
LDPE PL	5.7×10^4	~0	1.0×10^6	~0
AA	2.0×10^5	~0	1.2×10^6	~0
MET 0.5	9.4×10^4	~0	4.4×10^5	~0
MET 1	1.5×10^5	~0	2.4×10^5	0.3
MET 2	3.4×10^4	~0	4.7×10^5	~0
MET 5	2.9×10^4	~0	4.9×10^5	~0
MET 10	2.9×10^4	~0	4.7×10^5	~0
MET 20	3.6×10^4	~0	4.8×10^5	~0

overall antibacterial efficacy (R values) remained close to zero for both bacterial strains across all samples.

These findings confirm that metformin at concentrations achievable with our multistep process does not impart significant antibacterial activity. This result aligns with a few prior studies suggesting that metformin may not possess inherent antimicrobial capabilities, particularly when immobilized on polymeric substrates [9,10] (Table 4).

The apparent lack of antibacterial activity could be attributed to several factors. The metformin layer deposited on plasma-treated polyethylene using our multistep procedure might have been too thin or unstable to maintain prolonged contact with bacterial cells, thus reducing its potential impact. Additionally, the interaction dynamics between metformin and the bacterial cell walls may not be strong enough to induce cell membrane disruption or metabolic interference, mechanisms typically required for effective antibacterial action. For instance, Novita et al. demonstrated that metformin may boost the effectiveness of anti-tuberculosis treatments by promoting autophagy [11]. Furthermore, metformin has been shown to interact with the outer membrane of Gram-negative bacteria, effectively inhibiting the growth of *Klebsiella pneumoniae* [12]. In many studies, metformin exert rather adjuvant antimicrobial activity against Gram-positive and Gram-negative bacteria [61–63]. Other therapeutics which could fuel an interest in repurposing have been shown to exert some antimicrobial and anti-biofilm activities against clinically relevant bacteria [64,65]. Among them, heparin immobilized films showed a pronounced antibacterial effect toward the antibiotic-resistant *E. coli* K261 [66]. Indeed, the antibacterial efficacy cannot be directly compared with established antibacterial agents, such as chlorhexidine, which was deposited onto the surface in the same manner as metformin [67]. Metformin's indirect antimicrobial effect relies possibly on modulation of the host immune response, which is likely mediated through activation of the AMPK signaling pathway and subsequent induction of reactive oxygen species (ROS) in immune cells, contributing to disruption of bacterial metabolism [68,69].

Despite the limited success in achieving antibacterial activity, these results are crucial in highlighting the limitations of metformin as an antibacterial agent in surface modification applications. Future studies may explore alternative approaches to enhance the antimicrobial properties of such films. For instance, combining metformin with other antimicrobial agents, increasing the concentration of surface-immobilized metformin, or modifying the surface chemistry to improve the

interaction between the active substance and bacterial cells could yield more promising outcomes. Furthermore, additional tests, such as long-term exposure studies or the incorporation of metformin in multi-component polymer blends, could be considered. These modifications may help overcome the current limitations observed in this study and provide more comprehensive insights into the viability of metformin-functionalized surfaces for biomedical applications.

3.7. Evaluation of cytotoxicity

In vitro cytotoxicity was evaluated using the MTS assay as an indicator of mitochondrial succinate dehydrogenase enzyme activity. Cytotoxicity was classified based on the percentage of cell viability: values above 75% were considered non-cytotoxic, 75–50% indicated weak cytotoxicity, 50–25% represented moderate cytotoxicity, and values below 25% indicated strong cytotoxicity. The reference viability corresponds to 100% survival of cells in the absence of the tested substances in the culture medium. The cytotoxicity data are presented in Figure 7.

The obtained cytocompatibility data indicate that cell viability on the initial LDPE sample is almost 84%, which corresponds to non-cytotoxicity although the value is slightly lower than that of the control. The sample after treatment in low-temperature plasma has similar cytocompatibility. A somehow lower value is observed for the sample after incubation with the acrylic acid when the relative cell viability is around 72% what indicates weak cytotoxicity. Some deposited samples containing thin films based on metformin were non-cytotoxic, with values ranging from 99 to 97%, except for samples with metformin deposited from solutions with concentrations of 5, 10, and 20 $g{\cdot}L^{-1}$ ($p < 0.05$). For these samples, the relative cell viability dramatically decreases to the value of 21% for the sample deposited from the solution with concentration of 20 $g{\cdot}L^{-1}$ what indicates strong cytotoxicity. Strong cytotoxicity results in higher metformin concentrations suggest potential for anticancer treatment [70–72].

These findings are consistent with previous studies that demonstrated metformin's concentration-dependent effects on cellular viability and metabolic activity. Notably, Lei et al. demonstrated that metformin concentrations ranging from 0 to 500 µM enhanced the proliferation of human umbilical cord-derived mesenchymal stem cells (UCMSCs), whereas exposure to higher levels (1000 µM) led to an inhibitory effect [73]. In contrast, exposure of UCMSCs to higher metformin concentrations (0.1–50 mM) for 48 h led to a dose-dependent reduction in cell viability, with significant effects observed from 3 mM and maximal inhibition at 50 mM [74]. To assess the impact of exposure duration, BMSCs were treated with metformin (0.5–500 µM) for 14 days, resulting in a dose-dependent decline in cell viability, likely due to prolonged treatment reducing synthesis of factors, such as IGF-2 [75]. Biomaterial-based delivery systems have been shown to augment metformin's proliferative effects on MSCs. Ahmadi et al. showed that metformin-loaded mesoporous silica nanoparticles encapsulated in a hyaluronic acid/gelatin matrix enabled sustained release over 15 days, enhancing BMSC proliferation and metabolic activity, as confirmed by PicoGreen and MTT assays [76].

Therefore, while the cytotoxic response at high concentrations may restrict metformin's use in certain biomaterial settings, it also highlights the potential of

localized, concentration-dependent delivery systems in applications requiring controlled modulation of cell proliferation. Further investigation is warranted to better understand its mechanisms and optimize therapeutic efficacy across diverse physiological and pathological conditions.

4. Conclusion

This study successfully immobilized a very thin film of metformin onto LDPE surfaces through plasma treatment and carbodiimide chemistry, creating bioactive coatings with potential applications in biomedicine. The process involved air plasma treatment to introduce reactive oxygen and nitrogen groups, followed by grafting AA to provide some carboxyl groups for metformin attachment *via* EDC/NHS activation. FTIR confirmed the successful deposition of metformin, with characteristic N–H and C=N stretching peaks. Similar results were observed by XPS. The plasma treatment significantly improved the surface wettability, reducing the water contact angle from 82.6° (untreated LDPE) to 54.7° after metformin deposition at 0.5 g·L^{-1}. The WCA increased gradually with increasing metformin concentration. SEM/EDX analyses revealed surface heterogeneity and increased roughness due to stratified metformin layers, accompanied by N/O signals indicative of drug incorporation. Drug loading increased proportionally with incubation concentration, reaching up to ~72 µg per film for MET 20. *In vitro* release showed a biphasic profile—an initial burst followed by slower diffusion-limited release. Kinetic modeling revealed Korsmeyer–Peppas behavior (Fickian diffusion) at low loading (MET 1), while higher loadings (MET 5 and MET 20) followed first-order kinetics, suggesting concentration-dependent release from a surface-enriched matrix. The deviation from Higuchi assumptions reflects the non-uniform distribution and partial immobilization of the drug. Despite the surface modifications, antibacterial testing against *S. aureus* and *E. coli* showed no significant antibacterial activity. However, cytocompatibility assays using multipotent mesenchymal cells demonstrated that the metformin-coated surfaces exhibit interesting biocompatibility. A dose-dependent cytotoxicity was observed at higher metformin concentrations, with samples containing ≤5 g·L^{-1} metformin exhibiting minimal cytotoxicity, while higher concentrations led to reduced cell viability. Overall, the findings indicate that metformin-functionalized LDPE surfaces possess promising attributes for biomedical applications, where enhanced surface properties are critical. Building on these results, future research will aim to optimize these surfaces through combination therapies to enhance antimicrobial efficacy, thereby making metformin-functionalized coatings more suitable for advanced medical devices and therapeutic applications, including antibacterial and implant coatings. The combination of controlled release and localized cytotoxicity suggests that such systems could be tailored for site-specific therapeutic applications, where short-term cell inhibition is desired.

Author contributions

Conceptualization, Marián Lehocký, Kateřina Štěpánková, Pavel Sťahel, David Trunec, Miran Mozetič; methodology, Štěpán Žídek, Kateřina Štěpánková, Hana Pištěková, Milan Masař, Monika Stupavská; formal analysis and investigation, Marián Lehocký, Štěpán Žídek, Kateřina

Štěpánková, Hana Pišťěková, Monika Stupavská, David Trunec; writing–original draft preparation, Štěpán Žídek, Kateřina Štěpánková, Monika Stupavská, Pavel Sťahel, Miran Mozetič; funding acquisition, Marián Lehocký, Pavel Sťahel, David Trunec; resources, Marán Lehocký, Pavel Sťahel, David Trunec, Miran Mozetič; supervision, Marián Lehocký, Kateřina Štěpánková, David Trunec, Miran Mozetič.

Disclosure statement

No potential conflict of interest was reported by the author(s).

Funding

The work was supported by the Ministry of Education, Youth and Sports of the Czech Republic (RP/CPS/2024-28/005 and RP/CPS/2024-28/002). Author M. Mozetič greatly acknowledges the financial support from the Slovenian Research Agency, project L2-3163 'Development of safe multifunctional surfaces for catheters to combat biofilms' and core fund P2-0082. This research was also supported by project LM2023039 funded by the Ministry of Education, Youth and Sports of the Czech Republic. This work was supported from Operational Programme Johannes Amos Comenius OP JAC 'Application potential development in the field of polymer materials in the context of circular economy compliance (POCEK)', number CZ.02.01.01/00/23_021/0009004. This research was funded by Internal Grant Agency of Tomas Bata University in Zlín, Czech Republic (IGA/CPS/2025/005).

ORCID

Kateřina Štěpánková http://orcid.org/0000-0001-5290-3330

References

[1] Krishnamurthy N, Grimshaw AA, Axson SA, et al. Drug repurposing: a systematic review on root causes, barriers and facilitators. BMC Health Serv Res. 2022;22(1):970. doi: 10.1186/s12913-022-08272-z.

[2] Pinzi L, Bisi N, Rastelli G. How drug repurposing can advance drug discovery: challenges and opportunities. Front Drug Discov. 2024;4:1460100. doi: 10.3389/fddsv.2024.1460100.

[3] Kulkarni VS, Alagarsamy V, Solomon VR, et al. Drug repurposing: an effective tool in modern drug discovery. Russ J Bioorg Chem. 2023;49(2):157–166. doi: 10.1134/S1068162023020139.

[4] Center for Drug Evaluation and Research. U.S. Food and Drug Administration. Approved drug products with therapeutic equivalence evaluations. 41st ed. Silver Spring, MD: US Food and Drug Administration; 2021.

[5] Baker C, Retzik-Stahr C, Singh V, et al. Should metformin remain the first-line therapy for treatment of type 2 diabetes? Ther Adv Endocrinol Metab. 2021;12:2042018820980225. doi: 10.1177/2042018820980225.

[6] Marupuru S, Senapati P, Pathadka S, et al. Protective effect of metformin against tuberculosis infections in diabetic patients: an observational study of south Indian tertiary healthcare facility. Braz J Infect Dis. 2017;21(3):312–316. doi: 10.1016/j.bjid.2017.01.001.

[7] Plowman TJ, Christensen H, Aiges M, et al. Anti-inflammatory potential of the anti-diabetic drug metformin in the prevention of inflammatory complications and infectious diseases including COVID-19: a narrative review. Int J Mol Sci. 2024;25(10):5190. doi: 10.3390/ijms25105190.

[8] Martin DE, Cadar AN, Bartley JM. Old drug, new tricks: the utility of metformin in infection and vaccination responses to influenza and SARS-CoV-2 in older adults. Front Aging. 2023;4:1272336. doi: 10.3389/fragi.2023.1272336.
[9] Hossain S, Rafi RH, Ripa FA, et al. Modulating the antibacterial effect of the existing antibiotics along with repurposing drug metformin. Arch Microbiol. 2024;206(4):190. doi: 10.1007/s00203-024-03917-5.
[10] Masadeh MM, Alzoubi KH, Masadeh MM, et al. Metformin as a potential adjuvant antimicrobial agent against multidrug resistant bacteria. Clin Pharmacol. 2021;13:83–90. doi: 10.2147/CPAA.S297903.
[11] Novita BD, Ali M, Pranoto A, et al. Metformin induced autophagy in diabetes mellitus—tuberculosis co-infection patients: a case study. Indian J Tuberc. 2019;66(1):64–69. doi: 10.1016/j.ijtb.2018.04.003.
[12] Abbas H, Shaker G, Khattab R, et al. A new role of metformin as an efflux pump inhibitor in klebsiella pneumonia. J Microb Biotech Food Sci. 2021;11(1):e4232. doi: 10.15414/jmbfs.4232.
[13] Liu Y, Jia Y, Yang K, et al. Metformin restores tetracyclines susceptibility against multidrug resistant bacteria. Adv Sci. 2020;7(12):1902227. doi: 10.1002/advs.201902227.
[14] Moldasheva A, Surov V, Aljofan M. Editorial: new lights through old windows: metformin and derivatives as anti-cancer treatments. Front Pharmacol. 2022;13:889642. doi: 10.3389/fphar.2022.889642.
[15] Barczyński B, Frąszczak K, Kotarski J. Perspectives of metformin use in endometrial cancer and other gynaecological malignancies. J Drug Target. 2022;30(4):359–367. doi: 10.1080/1061186X.2021.2005072.
[16] Crist M, Yaniv B, Palackdharry S, et al. Metformin increases natural killer cell functions in head and neck squamous cell carcinoma through CXCL1 inhibition. J Immunother Cancer. 2022;10(11):e005632. doi: 10.1136/jitc-2022-005632.
[17] Song Y, Wu Z, Zhao P. The effects of metformin in the treatment of osteoarthritis: current perspectives. Front Pharmacol. 2022;13:952560. doi: 10.3389/fphar.2022.952560.
[18] Feng YY, Wang Z, Pang H. Role of metformin in inflammation. Mol Biol Rep. 2023;50(1):789–798. doi: 10.1007/s11033-022-07954-5.
[19] Kimber-Trojnar Ż, Dłuski DF, Wierzchowska-Opoka M, et al. Metformin as a potential treatment option for endometriosis. Cancers. 2022;14(3):577. doi: 10.3390/cancers14030577.
[20] Triggle CR, Marei I, Ye K, et al. Repurposing metformin for vascular disease. Curr Med Chem. 2023;30(35):3955–3978. doi: 10.2174/0929867329666220729154615.
[21] Song Y, Wu Z, Zhao P. The function of metformin in aging-related musculoskeletal disorders. Front Pharmacol. 2022;13:865524. doi: 10.3389/fphar.2022.865524.
[22] Alqahtani S, Mahzari M. Protective effect of metformin on venous thrombosis in diabetic patients: findings from a systematic review. J Endocrinol Metab. 2022;12(6):161–167. doi: 10.14740/jem848.
[23] Talebian S, Mendes B, Conniot J, et al. Biopolymeric coatings for local release of therapeutics from biomedical implants. Adv Sci. 2023;10(12):2207603. doi: 10.1002/advs.202207603.
[24] Ul Haq I, Krukiewicz K. Antimicrobial approaches for medical implants coating to prevent implants associated infections: insights to develop durable antimicrobial implants. Appl Surf Sci Adv. 2023;18:100532. doi: 10.1016/j.apsadv.2023.100532.
[25] Zhu G, Wang G, Jiao Li J. Advances in implant surface modifications to improve osseointegration. Mater Adv. 2021;2(21):6901–6927. doi: 10.1039/D1MA00675D.
[26] Xin H, Liu Y, Xiao Y, et al. Design and nanoengineering of photoactive antimicrobials for bioapplications: from fundamentals to advanced strategies. Adv Funct Mater. 2024;34(38):2402607. doi: 10.1002/adfm.202402607.
[27] Akdoğan E, Şirin HT. Plasma surface modification strategies for the preparation of antibacterial biomaterials: a review of the recent literature. Mater Sci Eng C Mater Biol Appl. 2021;131:112474. doi: 10.1016/j.msec.2021.112474.

[28] Petlin DG, Tverdokhlebov SI, Anissimov YG. Plasma treatment as an efficient tool for controlled drug release from polymeric materials: a review. J Control Release. 2017;266:57–74. doi: 10.1016/j.jconrel.2017.09.023.
[29] Booth J-P, Mozetič M, Nikiforov A, et al. Foundations of plasma surface functionalization of polymers for industrial and biological applications. Plasma Sources Sci Technol. 2022;31(10):103001. doi: 10.1088/1361-6595/ac70f9.
[30] Zhianmanesh M, Gilmour A, Bilek MMM, et al. Plasma surface functionalization: a comprehensive review of advances in the quest for bioinstructive materials and interfaces. Appl Phys Rev. 2023;10(2):021301. doi: 10.1063/5.0130829.
[31] Yılmazoğlu E, Karakuş S. Synthesis and specific biomedical applications of polymer brushes. Appl Surf Sci Adv. 2023;18:100544. doi: 10.1016/j.apsadv.2023.100544.
[32] Mozetič M. Aging of plasma-activated polyethylene and hydrophobic recovery of polyethylene polymers. Polymers. 2023;15(24):4668. doi: 10.3390/polym15244668.
[33] Bormashenko E, Chaniel G, Grynyov R. Towards understanding hydrophobic recovery of plasma treated polymers: storing in high polarity liquids suppresses hydrophobic recovery. Appl Surf Sci. 2013;273:549–553. doi: 10.1016/j.apsusc.2013.02.078.
[34] Štěpánková K, Ozaltin K, Pelková J, et al. Furcellaran surface deposition and its potential in biomedical applications. Int J Mol Sci. 2022;23(13):7439. doi: 10.3390/ijms23137439.
[35] Karakurt I, Ozaltin K, Pištěková H, et al. Effect of saccharides coating on antibacterial potential and drug loading and releasing capability of plasma treated polylactic acid films. Int J Mol Sci. 2022;23(15):8821. doi: 10.3390/ijms23158821.
[36] Štěpánková K, Ozaltin K, Sáha P, et al. Carboxymethylated and sulfated furcellaran from *Furcellaria lumbricalis* and its immobilization on PLA scaffolds. Polymers. 2024;16(5):720. doi: 10.3390/polym16050720.
[37] Schwarz DH, Elgaher WAM, Hollemeyer K, et al. Reversible immobilization of a protein to a gold surface through multiple host–guest interactions. J Mater Chem B. 2019;7(40):6148–6155. doi: 10.1039/c9tb00560a.
[38] dos Santos VLS, Araújo RC, Lisboa ES, et al. Layer-by-layer assembly: a versatile approach for tailored biomedical films and drug delivery. J Drug Deliv Sci Technol. 2024;91:105243. doi: 10.1016/j.jddst.2023.105243.
[39] Zhao C, Wen M, Wang Q, et al. Tailoring the corrosion resistance and biological performance of Mg-Zn-Y-Nd bioimplants with multiphasic, pore-sealed cerium-doped ceramic coatings via facile one-pot plasma electrolytic oxidation. J Mater Sci Technol. 2025;230:60–79. doi: 10.1016/j.jmst.2025.01.016.
[40] Jia Z, Hast K, Izgu EC. Catecholamine-copper redox as a basis for site-specific single-step functionalization of material surfaces. ACS Appl Mater Interfaces. 2021;13(3):4711–4722. doi: 10.1021/acsami.0c19396.
[41] Hast K, Stone MRL, Jia Z, et al. Bioorthogonal functionalization of material surfaces with bioactive molecules. ACS Appl Mater Interfaces. 2023;15(4):4996–5009. doi: 10.1021/acsami.2c20942.
[42] Ozaltin K, Lehocký M, Kuceková Z, et al. A novel multistep method for chondroitin sulphate immobilization and its interaction with fibroblast cells. Mater Sci Eng C Mater Biol Appl. 2017;70(Pt 1):94–100. doi: 10.1016/j.msec.2016.08.065.
[43] Adeli F, Abbasi F, Babazadeh M, et al. Thermo/pH dual-responsive micelles based on the host–guest interaction between benzimidazole-terminated graft copolymer and β-cyclodextrin-functionalized star block copolymer for smart drug delivery. J Nanobiotechnol. 2022;20(1):91. doi: 10.1186/s12951-022-01290-3.
[44] Ozaltin K, Lehocký M, Humpolíček P, et al. A new route of fucoidan immobilization on low density polyethylene and its blood compatibility and anticoagulation activity. Int J Mol Sci. 2016;17(6):908. doi: 10.3390/ijms17060908.
[45] Mussano F, Lee KJ, Zuk P, et al. Differential effect of ionizing radiation exposure on multipotent and differentiation-restricted bone marrow mesenchymal stem cells. J Cell Biochem. 2010;111(2):322–332. doi: 10.1002/jcb.22699.

[46] Honda Y, Ding X, Mussano F, et al. Guiding the osteogenic fate of mouse and human mesenchymal stem cells through feedback system control. Sci Rep. 2013;3(1):3420. doi: 10.1038/srep03420.
[47] Sabbagh BA, Kumar PV, Chew YL, et al. Determination of metformin in fixed-dose combination tablets by ATR-FTIR spectroscopy. Chem Data Collect. 2022;39:100868. doi: 10.1016/j.cdc.2022.100868.
[48] Agnes C, Perveen N, Khan NH, et al. Quantitative determination of metformin hydrochloride tablet of different brands available in Malaysia by UV spectrophotometry and Fourier transform infrared spectroscopy (FTIR). BJSTR. 2022;46(3):37387–37401. doi: 10.26717/BJSTR.2022.46.007345.
[49] van Oss CJ, Wu W, Docoslis A, et al. The interfacial tensions with water and the Lewis acid–base surface tension parameters of polar organic liquids derived from their aqueous solubilities. Colloids Surf B Biointerfaces 2001;20(1):87–91. doi: 10.1016/s0927-7765(00)00169-7.
[50] Suresh B, Maruthamuthu S, Kannan M, et al. Mechanical and surface properties of low-density polyethylene film modified by photo-oxidation. Polym J. 2011;43(4):398–406. doi: 10.1038/pj.2010.147.
[51] Primc G, Mozetič M. Hydrophobic recovery of plasma-hydrophilized polyethylene terephthalate polymers. Polymers. 2022;14(12):2496. doi: 10.3390/polym14122496.
[52] Primc G, Mozetič M. Surface modification of polymers by plasma treatment for appropriate adhesion of coatings. Materials. 2024;17(7):1494. doi: 10.3390/ma17071494.
[53] Che C, Dashtbozorg B, Qi S, et al. The ageing of μplasma-modified polymers: the role of hydrophilicity. Materials. 2024;17(6):1402. doi: 10.3390/ma17061402.
[54] Peršin Fratnik Z, Plohl O, Kokol V, et al. Using different surface energy models to assess the interactions between antiviral coating films and phi6 model virus. J Funct Biomater. 2023;14(4):232. doi: 10.3390/jfb14040232.
[55] E. Abusrafa A, Habib S, Krupa I, et al. Modification of polyethylene by RF plasma in different/mixture gases. Coatings. 2019;9(2):145. doi: 10.3390/coatings9020145.
[56] Jokinen V, Suvanto P, Franssila S. Oxygen and nitrogen plasma hydrophilization and hydrophobic recovery of polymers. Biomicrofluidics. 2012;6(1):016501. doi: 10.1063/1.3673251.
[57] Alibolandi M, Sadeghi F, Abnous K, et al. The chemotherapeutic potential of doxorubicin-loaded PEG-b-PLGA nanopolymersomes in mouse breast cancer model. Eur J Pharm Biopharm. 2015;94:521–531. doi: 10.1016/j.ejpb.2015.07.005.
[58] Askarizadeh M, Esfandiari N, Honarvar B, et al. Kinetic modeling to explain the release of medicine from drug delivery systems. ChemBioEng Rev. 2023;10(6):1006–1049. doi: 10.1002/cben.202300027.
[59] Shafiei F, Ghavami-Lahiji M, Jafarzadeh Kashi TS, et al. Drug release kinetics and biological properties of a novel local drug carrier system. Dent Res J. 2021;18(1):94. doi: 10.4103/1735-3327.330875.
[60] Mir A, Fletcher WJ, Taylor DK, et al. Sustained release studies of metformin hydrochloride drug using conducting polymer/gelatin-based composite hydrogels. ACS Omega. 2024;9(17):18766–18776. doi: 10.1021/acsomega.3c05067.
[61] He X, Jin S, Fan W, et al. Synergistic *in vitro* antimicrobial activity of Triton X-100 and metformin against *Enterococcus faecalis* in normal and high-glucose conditions. Microorganisms. 2022;10(1):124. doi: 10.3390/microorganisms10010124.
[62] Wu X, Fan W, Fan B. Synergistic effects of silver ions and metformin against *Enterococcus faecalis* under high-glucose conditions *in vitro*. BMC Microbiol. 2021;21(1):261. doi: 10.1186/s12866-021-02291-2.
[63] Attia HG, Albarqi HA, Said IG, et al. Synergistic effect between amoxicillin and zinc oxide nanoparticles reduced by oak gall extract against *Helicobacter pylori*. Molecules. 2022;27(14):4559. doi: 10.3390/molecules27144559.

[64] Parfenova LV, Galimshina ZR, Gil'fanova GU, et al. Hyaluronic acid bisphosphonates as antifouling antimicrobial coatings for PEO-modified titanium implants. Surf Interfaces. 2022;28:101678. doi: 10.1016/j.surfin.2021.101678.
[65] Leme RCP, Silva RB da. Antimicrobial activity of non-steroidal anti-inflammatory drugs on biofilm: current evidence and potential for drug repurposing. Front Microbiol. 2021;12:707629.
[66] Permyakova ES, Kiryukhantsev-Korneev PV, Ponomarev VA, et al. Antibacterial activity of therapeutic agent-immobilized nanostructured TiCaPCON films against antibiotic-sensitive and antibiotic-resistant *Escherichia coli* strains. Surf Coat Technol. 2021;405:126538. doi: 10.1016/j.surfcoat.2020.126538.
[67] Ozaltin K, Di Martino A, Capakova Z, et al. Plasma mediated chlorhexidine immobilization onto polylactic acid surface via carbodiimide chemistry: antibacterial and cytocompatibility assessment. Polymers. 2021;13(8):1201. doi: 10.3390/polym13081201.
[68] Goel S, Singh R, Singh V, et al. Metformin: activation of 5′ AMP-activated protein kinase and its emerging potential beyond anti-hyperglycemic action. Front Genet. 2022;13:1022739. doi: 10.3389/fgene.2022.1022739.
[69] Kajiwara C, Kusaka Y, Kimura S, et al. Metformin mediates protection against Legionella pneumonia through activation of AMPK and mitochondrial reactive oxygen species. J Immunol. 2018;200(2):623–631. doi: 10.4049/jimmunol.1700474.
[70] Mahfauz M, Yuruker O, Kalkan R. Repurposing metformin as a potential anticancer agent using *in silico* technique. Daru. 2024;32(2):549–555. doi: 10.1007/s40199-024-00523-0.
[71] Jinadasa AGRG, Akalanka HMK, Wageesha NDA, et al. Metformin as a potential *in vitro* anticancer modulator of adenosine monophosphate kinase: a review. Int J Breast Cancer. 2024;2024(1):1094274. doi: 10.1155/2024/1094274.
[72] Raafat SN, El Wahed SA, Badawi NM, et al. Enhancing the anticancer potential of metformin: fabrication of efficient nanospanlastics, *in vitro* cytotoxic studies on HEP-2 cells and reactome enhanced pathway analysis. Int J Pharm X. 2023;6:100215. doi: 10.1016/j.ijpx.2023.100215.
[73] Lei T, Deng S, Chen P, et al. Metformin enhances the osteogenesis and angiogenesis of human umbilical cord mesenchymal stem cells for tissue regeneration engineering. Int J Biochem Cell Biol. 2021;141:106086. doi: 10.1016/j.biocel.2021.106086.
[74] Bajetto A, Pattarozzi A, Sirito R, et al. Metformin potentiates immunosuppressant activity and adipogenic differentiation of human umbilical cord-mesenchymal stem cells. Int Immunopharmacol. 2023;124(Pt B):111078. doi: 10.1016/j.intimp.2023.111078.
[75] Montazersaheb S, Kabiri F, Saliani N, et al. Prolonged incubation with metformin decreased angiogenic potential in human bone marrow mesenchymal stem cells. Biomed Pharmacother. 2018;108:1328–1337. doi: 10.1016/j.biopha.2018.09.135.
[76] Ahmadi S, Dadashpour M, Abri A, et al. Long-term proliferation and delayed senescence of bone marrow-derived human mesenchymal stem cells on metformin co-embedded HA/Gel electrospun composite nanofibers. J Drug Deliv Sci Technol. 2023;80:104071. doi: 10.1016/j.jddst.2022.104071.